Plant Science 256 (2017) 53–64

Contents lists available at ScienceDirect

Plant Science

journal homepage: www.elsevier.com/locate/plantsci

Apple autophagy-related protein MdATG3s afford tolerance to multiple abiotic stresses

Ping Wang [1,2], Xun Sun [1], Xin Jia, Fengwang Ma *

State Key Laboratory of Crop Stress Biology for Arid Areas, College of Horticulture, Northwest A&F University, Yangling, Shaanxi 712100, China

ARTICLE INFO

Article history:
Received 25 September 2016
Received in revised form
28 November 2016
Accepted 8 December 2016
Available online 15 December 2016

Keywords:
Abiotic stress
Apple
ATG3
Arabidopsis
Autophagy
Overexpression

ABSTRACT

The efficient degradation system of autophagy in plant cells has important roles in removing and recycling intracellular components during normal development or under environmental stresses. Formation of autophagosomes requires the conjugation of ubiquitin-like protein ATG8 to phosphatidylethanolamine (PE). We isolated two ubiquitin-conjugating enzyme E2-like *ATG3* homologues from *Malus domestica* – *MdATG3a* and *MdATG3b* – that are crucial for ATG8-PE conjugation. Both share a conserved N-terminal, as well as the catalytic and C-terminal domains of ATG3 with HPC and FLKF motifs. Each promoter was isolated from genomic DNA and contained several *cis*-acting elements that are involved in responses to environmental stresses or hormones. In addition to having the same cellular localization in the nucleus and cytoplasm, *MdATG3a* and *MdATG3b* showed similar expression patterns toward leaf senescence, nitrogen starvation, drought, salinity, and oxidative stress at the transcriptional level. Ectopic expression of either in *Arabidopsis* conferred tolerance to osmotic or salinity stress and also improved growth performance under nitrogen- or carbon-starvation. Callus lines of 'Orin' apple that over-expressed *MdATG3b* also displayed better growth performance when nutrient supplies were limited. These overall results demonstrate that, as important autophagy genes, overexpression of *MdATG3s* can afford tolerance to multiple abiotic stresses at the cellular and whole-plant level.

1. Introduction

Global climate changes are threatening agriculture due to great pressures from human population growth and industrialization. Increased attention by farmers, scientists, and policy makers is needed to sustain productivity and future crop cultivation. Environmental hazards can reduce plant quality, yields, and biomass production [1]. Common abiotic challenges include drought, salt, oxidative, and nutrient stresses that arise from water shortages, ion toxicity, reactive oxidative species (ROS) bursts, nitrogen (N) depletion in the soil, or carbon (C) deficiencies. Under such adverse conditions, plant cells undergo rapid fluctuations to adapt their metabolism and protect themselves against potential damage. This involves the concerted action of diverse stress-response pathways at the cellular or physiological level. One key cellular pathway that mediates stress-induced metabolic adaptations and damage control is macroautophagy (hereafter, 'autophagy').

Autophagy is a conserved biological process that entails the degradation of cytoplasmic organelles or cytosolic components for recycling in eukaryotic cells [2]. Cellular autophagy begins with the formation of double-membraned vesicles and autophagosomes, which then sequester proteins or organelles or portions of the cytoplasm for delivery to the lysosome or vacuole. The process ends with the degradation of these components and recycling to maintain nutrient and energy homeostasis [3]. It comprises four steps: induction and cargo selection, nucleation and expansion, docking and fusion, and breakdown and export [4]. Researchers have identified and characterized more than 30 autophagy-related genes (*ATG*s) in yeast by genetic screening [4,5]. Homologues and functions for many of those genes have now been characterized in mammalian species [6] and plants [7,8]. The relevant proteins fall into several functional groups, including ATG1 kinase complex, ATG2/9/18 transmembrane complex, phosphatidylinositol 3-kinase (PI3 K) complex, and two ubiquitin-like protein (ATG8 and ATG12) conjugation systems [5]. Both conjugation systems are essential for the biogenesis of membrane isolation and expansion. The ATG8-PE system is required for autophagosome transport and maturation, as well as for the specific selection of autophagic cargo

* Corresponding author.
E-mail addresses: fwm64@sina.com, fwm64@nwsuaf.edu.cn (F. Ma).
[1] These authors contributed equally to this work.
[2] Present address: Department of Genetics, Development and Cell Biology, Iowa State University, Ames, IA 50010, USA.

http://dx.doi.org/10.1016/j.plantsci.2016.12.003
0168-9452/

[2]. For conjugation to PE, ATG8 with a C-terminal glycine residue is activated by ATG7 (E1-like) and transferred to ATG3 (E2-like). *In vitro* reconstitution studies have revealed that ATG3, ATG7, ATG8, ATP, and PE-containing membranes are necessary for this conjugation of ATG8 with PE [9]. Although most E2 enzymes require E3 enzymes, ATG3 itself is catalytically competent for ATG8-PE formation [10].

Nitrogen depletion and carbon starvation are the most potent physiological stimuli that induce autophagy. Various *Arabidopsis atg*-mutants, e.g., *atg7-1*, *atg9-1*, *atg4a4b-1*, *atg5-1*, and *atg10-1*, are hypersensitive to nutrient-limiting conditions [11]. Transcripts of some *AtATG*s can be induced during sucrose starvation in a coordinated manner [12]. Exposure to oxidative stress can also stimulate autophagy via ROS accumulations [13] or protein oxidization [14,15]. In *Arabidopsis*, salinity or osmotic stress can activate autophagy by up-regulating *AtATG18a* expression; *AtATG18a* RNAi plants exhibit hypersensitivity to these two stresses [16]. *Arabidopsis AtATG8f* and *OsATG10b* from *Oryza sativa* (rice) also function in responses to salt and osmotic stresses [17,18]. In addition to these abiotic challenges, autophagy plays a unique role in responses to endoplasmic reticulum (ER) stress [19,20] and high temperatures [21,22].

As one of the most economically important fruits worldwide, production of *Malus domestica* (apple) is limited by various environmental stresses in the main cultivation area of northwestern China, a region that experiences frequent water deficits and depletion of soil nutrients. Because autophagy has important roles in abiotic-stress responses, especially during periods of limited nutrient availability, we focus on the function studies of core *ATG* genes in apple, with emphasis on the necessary genes for ATG8-PE conjugation system. Previously, we isolated and characterized two important apple genes in the ATG8-PE conjugation system – *MdATG8i* [23] and *MdATG7s* [24]. We have found that they were induced transcriptionally by various abiotic stresses and their overexpression led to improved tolerance to nutrient starvation in *Arabidopsis* or apple callus [23,24]. Given that ATG3 catalyzes protein–lipid conjugation and is essential for the interaction with PE in the ATG8-PE conjugation system [25], we suppose that ATG3 works with ATG8 and ATG7 in a synergetic way and might also have a potential to improve abiotic stress tolerance. To prove that assumption, in this study, we isolated and explored the functions of *ATG3s* from apple, and tested their roles in abiotic stresses when over-expressed in *Arabidopsis* and apple calli. Their expression patterns and phenotype of transgenic plants in response to abiotic stresses indicated the potential and importance in stress tolerance improvement.

2. Materials and methods

2.1. Plant materials and treatments

Two-year-old plants of *Malus domestica* Borkh. cv. Golden Delicious were produced by grafting onto *M. hupehensis* in the greenhouse at the Horticultural Experimental Station of Northwest A&F University, Yangling, China. Leaves were marked as they emerged and samples were collected at different ages (from fully mature to yellow) to analyze expression patterns during the senescence process. Fully mature leaves were used for cloning *MdATG3*s and their promoter regions, as well as for performing a detachment treatment under darkness to induce senescence, as previously described [26].

For analyzing expression in various tissue types, we obtained buds, young shoots, stems, flowers, white roots, well-developed fruits, and mature leaves from three eight-year-old 'Golden Delicious' trees growing at the Horticultural Experimental Station of Northwest A&F University [23].

Seedlings of *M. hupehensis* Rehd. growing in sand-filled pots were used for stress treatments. To simulate N-depletion, we watered approximately five-month-old seedlings with Hoagland's nutrient solution in which $Ca(NO_3)_2$ and KNO_3 were replaced by $CaCl_2$ and KCl for 45 d. Control plants continued to receive the standard solution. For studying the effects of treatment with methyl viologen (MV), salinity (excess NaCl), or dithiothreitol (DTT), three-month-old seedlings were transferred to hydroponic culturing conditions [27]. The MV, NaCl, or DTT were added to individual Hoagland solutions to obtain final concentrations of 50 μM, 200 mM, or 3 mM, respectively. For drought treatment, three-month-old seedlings were transferred to soil and grown for another two months before they were progressively stressed by withholding normal irrigation for 10 d [28]. The leaves or roots from five seedlings per treatment were sampled for RNA isolations.

For phenotyping transgenic *Arabidopsis* during a normal growth period or in response to abiotic stress, wild-type (WT; Col-0) and two homozygous T_3 transgenic lines from each gene were used. Morphological comparisons were made after sowing WT and T_3 seeds in soil and exposing the seedlings to long-day conditions (LD; 16-h photoperiod). Plants were photographed and the maximum radius of a rosette was measured with an electronic digital caliper on indicated days. Other seeds were sterilized and germinated on a standard MS medium. The resultant seedlings were exposed to LD conditions, and bolting time was recorded as the time at which the main inflorescence shoot had elongated to 5 mm long [29]. Photographs were taken at 25 d. In a separate examination, 7-day-old uniformly sized seedlings were transferred for 15 d to either standard MS plates or those supplemented with 200 mM mannitol or 100 mM NaCl. For testing the effects of N-starvation on *Arabidopsis*, 5-day-old uniformly sized seedlings were transferred to MS control, N-depleted and N/Sugar-depleted agar plates and treated as described previously [23]. Plants were photographed at 10 d and 25 d under a light microscope (DM2000; Leica, Germany), and fresh weights and root lengths were recorded after 10 d. Our C-starvation treatment also followed the method previously described [23]. As an alternative test of C-starvation effects, seeds were sterilized and germinated on standard MS agar media under LD conditions. After 14 d, the plates were wrapped with aluminum foil and incubated under darkness for another 14 d. Seedlings were photographed every other day to record growth recovery after they were returned to the LD scenario [30].

Transgenic and WT 'Orin' apple calli were used to investigate growth responses to C- or N-deficiencies, based on treatments previously described [23]. Similarly, 0.02-g portions of 10-day-old calli were transferred to the following treatment media for 20 d: (1) MS control; (2) Low-sugar, with the sucrose concentration reduced from 30 g L^{-1} to 3 g L^{-1}; or (3) Low-nitrogen, with the N concentration decreased from 60 mM to 5 mM.

2.2. RNA extraction, cloning, and real-time PCR

After total RNA was extracted by the CTAB method [31], residual DNA was digested by RNase-free DNase I (Invitrogen, Carlsbad, CA, USA). First-strand cDNA was synthesized using the RevertAid™ First Strand cDNA synthesis kit (Fermentas, Thermo Scientific, Waltham, MA, USA), all according to the manufacturers' protocols. Using *Arabidopsis ATG3* (AT5G61500) amino acid sequence against the genome database of *M. domestica* (https://www.rosaceae.org/species/malus/all), two homologues were predicted and thus specific primers were designed. The coding sequences (CDS) of *MdATG3*s were amplified by high-fidelity Platinum *Taq* DNA Polymerase (Invitrogen). Quantitative real-time

PCR was performed as previously described [23]. Specific primers and sequences are listed in Supplementary Table 1.

2.3. Genomic DNA extraction and promoter isolation

Genomic DNA was extracted by an improved CTAB method [32], and PCR was performed with high-fidelity Platinum *Taq* DNA Polymerase, using specific primers for cloning promoter regions (Supplementary Table 1). The PCR-amplified fragments were sequenced by Invitrogen Biotechnology Co., Ltd. (Shanghai, http://www.invitrogen.com.cn).

2.4. Sequence analysis

Sequence alignments with homologues from other species were done by DNAMAN. Putative conserved domains were predicted by Pfam (http://pfam.xfam.org/) and InterPro (https://www.ebi.ac.uk/interpro/). The *cis*-acting elements in the promoters were predicted by the PlantCARE program (http://bioinformatics.psb.ugent.be/webtools/plantcare/html/).

2.5. Subcellular localizations

The CDS of *MdATG3*s were amplified with primers with *Xba*I and *Kpn*I sites (Supplementary Table 1), and the stop codon was removed for green fluorescence protein (GFP) fusion expression at the C-terminus. The PCR product was cloned into the pMD19-T simple vector (Takara, Kyoto, Japan) and sequenced. Both the pMD19-T plasmid and empty vector pBI221 (CaMV35S promoter and GFP tag) were double-digested with *Xba*I and *Kpn*I, then ligated by T4 ligase (Takara). Sequence-confirmed plasmids were transiently transformed into onion epidermal cells with a gene gun (Bio-Rad, Hercules, CA, USA), using the pBI221 empty vector as the control. After bombardment, the cells were cultured in an MS medium in the dark at 22 °C for 20 h before being observed under a confocal microscope (Zeiss LSM, Minneapolis, MN, USA).

2.6. Yeast two-hybrid (Y2H) assays

Using the *MdATG8i*-pGBKT7 plasmid and a protocol similar to that previously described [23], we separately cloned the CDS of *MdATG3a* and *MdATG3b* into the pGADT7 vector (Clontech Laboratories, Inc., http://www.clontech.com/), using primers with restriction sites (Supplementary Table 1). The constructs were co-transformed into yeast strain AH109 according to the Clontech protocol. Protein–protein interactions were examined by checking the growth and color of transformed colonies on SD-Leu-Trp and SD-Leu-Trp-His-Ade + X-α-gal plates.

2.7. Complementation assay in yeast *atg3*△ mutant

For yeast expression, the CDS of *MdATG3a* and *MdATG3b* were recombined into the pYES2 vector (Invitrogen) by *Kpn*I and *Eco*RI double digestion. Primers were listed in Supplementary Table 1. The pYES2-*MdATG3a* and −*MdATG3b* constructs and pYES2 empty vector were respectively transformed into the yeast *atg3*△ mutant cells (Invitrogen; BY4741, *atg3*△:*kanMX*, *MATa*; *his3*△*1*; *leu2*△*0*; *met15*△*0*; *ura3*△*0*) according to the Clontech protocol. Transformants were selected on SD-Ura plates and confirmed by PCR. Wild type (WT) S288C and *atg3*△ mutant cells were cultured in YPDA with 2% glucose, while yeast cells with positive transformants were cultured in YPDA with 2% galactose instead of glucose. Yeast cells were harvested when the OD600 reached 0.5, and washed three times with water. Then they were re-suspended in N-depleted medium (0.17% yeast nitrogen base without ammonium sulfate and amino acids but plus 2% galactose or 2% glucose) to induce N-starvation. After 18 d, streak the starved yeast cells on nutrient-rich YPDA plates for recovery [33].

2.8. Generation of transgenic arabidopsis thaliana plants

The Gateway binary vector pGWB405, with a GFP fusion at the C-terminus under control of the CaMV35S promoter, was used for constructing a plant overexpression vector of *MdATG3a*. Following the Gateway Technology protocol (Invitrogen), *MdATG3a* was inserted into pGWB405 destination vector by the reactions of BP and LR clonase enzymes (Invitrogen), using pDONR222 as the donor vector. Because pGWB405 did not, for some unknown reason, work successfully for *MdATG3b* during vector construction, we inserted the gene into another binary vector, pCambia 2300 (CaMV35S promoter, no tag), using double-digestion with *Bam*HI and *Kpn*I. Primers are listed in Supplementary Table 1. Sequence-confirmed plasmids were transformed into *Agrobacterium tumefaciens* strain EHA105 by electroporation. Transformation into *Arabidopsis* plants was performed according to the floral-dip procedure [34]. All growth conditions and the procedure for selecting homozygous T_3 transgenic plants matched those previously described [23].

2.9. Generation of MdATG3b-transgenic 'Orin' apple callus

A. tumefaciens EHA105 carrying the *MdATG3b*-pCambia2300 plasmid was transformed into 'Orin' apple callus following the protocol previously specified [35]. 'Orin' apple callus grew on an MS agar medium containing 1.0 mg L^{-1} 2,4-D and 1.0 mg L^{-1} 6-BA in the dark at 25 °C, and sub-cultured at 15-d intervals. Seven-day-old callus grown in a liquid medium were used for transformation by infection with Agrobacterium (10 min, gentle rotation, 25 °C). After 2 d co-cultivation, the callus was washed three times with sterile water containing 400 mg L^{-1} cefotaxime, then transferred to a subculture medium supplemented with 200 mg L^{-1} cefotaxime and 30 mg L^{-1} kanamycin for transgene selection [35].

2.10. Statistical analysis

Data are shown with values expressed as means and standard deviation (SD). Statistical differences were compared by Student's *t*-tests at significance levels of $P < 0.05$ (*), $P < 0.01$ (**), or $P < 0.001$ (***).

3. Results

3.1. Molecular cloning, sequence analysis, and subcellular localization of MdATG3s

Through homology-cloning, we obtained two homologous *AtATG3* genes (TAIR: AT5G61500) from *Malus domestica* and named them *MdATG3a* (GenBank Accession No. KF438032) and *MdATG3b* (GenBank Accession No. KR024682). Each contains a 927-bp open reading frame and encodes 308 amino acid-deduced proteins. They share over 98% similarity in their nucleotide sequences and amino acids. Sequence alignment with AtATG3 and OsATG3 revealed 85.31% similarity plus conserved HPC and FLKF motifs (Fig. 1A). Just before the FLKF motif, there is a conserved DKYLFL motif between apple and *Arabidopsis* (Fig. 1A). Both MdATG3a and MdATG3b comprise three characteristic domains: N-terminal domain, catalytic domain, and the C-terminal domain of autophagy-related protein 3 (Fig. 1B). The N-terminal domain has 123 amino acid residues and extends from Position 7–129, while the catalytic domain has 61 amino acid residues that span positions from 194 to 254. The conserved cysteine residue (Cys^{253}) within the HPC motif is a putative

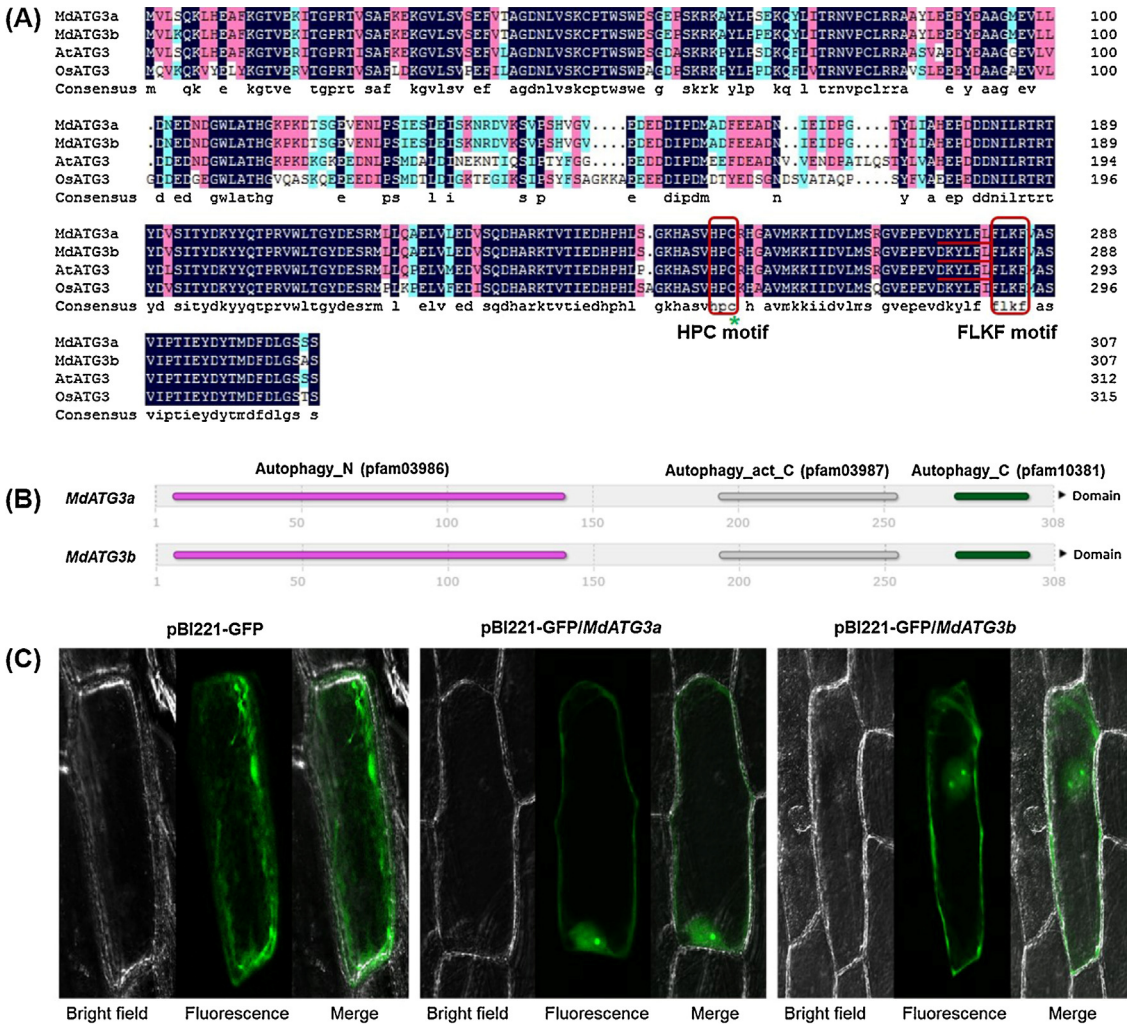

Fig. 1. Sequence analysis and cellular localization of MdATG3s. (A) Alignment of deduced amino acid sequences of MdATG3a and MdATG3b with AtATG3 (NP_568934.1) and OsATG3 (XP_015613678.1). Red boxes indicate HPC and FLKF motifs. Red underlines indicate DKYLFL motif conserved between apple and *Arabidopsis*. *, conserved cysteine residue. (B) Conserved domains within MdATG3a and MdATG3b. (C) Subcellular localization analysis of MdATG3a–and MdATG3b–GFP fusion protein in onion epidermal cells. (For interpretation of the references to colour in this figure legend, the reader is referred to the web version of this article.)

active-site residue that is unique to autophagic E2 enzymes, including both ATG3 and ATG10 [36]. Finally, the small C-terminal domain consists of 25 amino acid residues between Positions 275 and 299, and it contains a highly characteristic conserved FLKF motif.

To investigate the subcellular localization of MdATG3a and MdATG3b, we fused them individually with GFP at the C-terminus for transient expression in onion epidermal cells under the control of the CaMV35S promoter. Our fluorescence observations indicated the presence of either MdATG3a– or MdATG3b–GFP fusion protein in the cytoplasm and nucleus of the cells (Fig. 1C).

3.2. Promoter cloning and analysis

Although *MdATG3a* and *MdATG3b* proved highly similar, they were predicted to be located on different apple chromosomes, with *MdATG3a* in contig MDC017858.191 of Chromosome 6 and *MdATG3b* in contig MDC003928.273 of Chromosome 7. To get more information on *MdATG3s*, their promoters were cloned and in silico analyzed by PlantCARE online program. A 1427-bp fragment (GenBank Accession No. KX790786) was identified upstream of the *MdATG3a* CDS region, while a 1764-bp fragment (GenBank Accession No. KX790787) was isolated upstream of the *MdATG3b* CDS region. Analysis of the *cis*-acting elements revealed that both promoters were rich in elements involved in responses to environmental stresses (MBS, TC-rich repeats, and HSE) as well as to hormones. The latter included GARE-motif (GA-responsive), TCA-element (SA-responsive), and CGTCA/TGACG-motif (MeJA-responsive) (Fig. 2A, B; Supplementary Table 2). Within their promoter regions, common *cis*-regulatory elements required for endosperm expression (Skn-1_motif) or involved in circadian control (Circadian) were also identified (Fig. 2A, B; Supplementary Table 2). In addition, an ethylene-responsive element (ERE) and a CCGTCC-box related to meristem-specific activation were found in the *MdATG3a* promoter region, while a W-box for fungal elicitor-responsiveness and an ARE motif essential for anaerobic induction occurred in the *MdATG3b* promoter region (Fig. 2A, B; Supplementary Table 2).

3.3. Expression analysis of MdATG3s

The mRNAs of *MdATG3a* and *MdATG3b* were expressed in all tested apple tissues, including buds, shoots, stems, flowers, fruits, roots, and leaves. Although well-developed fruits had relatively high levels of transcripts for both genes, *MdATG3b* was more strongly expressed than *MdATG3a* in mature leaves (Fig. 3A). Transcripts were also detected from two different types of leaf

Fig. 2. Putative *cis*-acting elements (shaded in gray) in promoter regions of *MdATG3s*, as predicted by PlantCARE database. (A) A 1427-bp fragment of *MdATG3a* promoter (GenBank Accession No. KX790786). (B) A 1764-bp fragment of *MdATG3b* promoter (GenBank Accession No. KX790787). Key sequence elements – TATA box and CAAT box – are shaded in green and dark yellow, respectively. Letters in red indicate start codon ATG for *MdATG3a* and *MdATG3b*. (For interpretation of the references to colour in this figure legend, the reader is referred to the web version of this article.)

senescence. In dark-induced senescence of detached leaves, transcript levels gradually increased by 4.1-fold for *MdATG3a* at Day 15 and by 2.5-fold for *MdATG3b* at Day 10. *MdATG3a* was overall more highly expressed during such treatment (Fig. 3B). In age-dependent natural leaf senescence, transcript levels for both genes increased abundantly in older leaves. For example, in 185-day-old leaves, increments of 14-fold and 26-fold were found for *MdATG3a* and *MdATG3b*, respectively. Overall, *MdATG3b* was more strongly expressed than *MdATG3a* during natural leaf senescence (Fig. 3C).

We also examined *MdATG3s* expression in apple plants under abiotic stress. In response to N-starvation for 45 d, expression patterns differed between genes, with *MdATG3a* transcript levels remaining unchanged in the first 36 d of treatment before increasing by 3-fold over the control at Day 45 (Fig. 3D). By comparison, *MdATG3b* responded earlier, with transcript levels rising by 2.6-fold in the first 18 d, followed by smaller increments relative to the control (Fig. 3D). When oxidative stress was induced by applying MV to the roots, increases in root mRNA levels for *MdATG3a* and *MdATG3b* were similar, showing respective increments of 16.3-fold and 8.8-fold at 9 h. Overall, *MdATG3a* was more highly expressed than *MdATG3b* in response to MV treatment (Fig. 3E). Similar trends in leaf samples were noted from our drought and salinity treatments. For example, after 8 d of drought treatment, *MdATG3a* and *MdATG3b* were up-regulated by 8.7-fold and 3.8-fold, respectively, when compared with measurements made at Day 0 (Fig. 3F). After 8 h of exposure to 200 mM NaCl, *MdATG3a* and *MdATG3b* were up-regulated by 1.9-fold and 4.1-fold, respectively (Fig. 3G). Applying 3 mM DTT to the roots to induce ER stress caused *MdATG3a* and *MdATG3b* in roots to be up-regulated by 6.1-fold and 15.6-fold, respectively, after 12 h of treatment (Fig. 3H).

These results demonstrated that *MdATG3a* and *MdATG3b* had similar expression patterns in different tissues and in response to most treatments, including leaf senescence, N-depletion, oxidative stress, drought, salinity, and ER stress. Thus, we might infer that the two genes have similar functions, based on the closeness of their sequences and expression patterns.

3.4. *MdATG3s interact with MdATG8i in yeast and could complement atg3△ yeast mutant under N starvation*

Since the conjugation of ATG8 to PE needs sequential activation by E1-like ATG7 and E2-like ATG3, there are interactions between ATG8 and ATG7 or ATG3 [9,10,25]. Previously, we identified the interaction of MdATG8i with MdATG7s in yeast [23]. To test whether MdATG3s interact with MdATG8i, Y2H was performed using the MdATG8i-pGBKT7 as bait and MdATG3a/3b-pGADT7 as preys. Fig. S1 showed that both MdATG3a or MdATG3b could interact with MdATG8i in yeast, implying the conserved participation of MdATG3s in the ATG8-PE conjugation system. To test if the homologs of *ATG3* from apple could complement *atg3*△ yeast mutant, *MdATG3a* and *MdATG3b* were constructed to a yeast expression vector pYES2. After N starvation, the *atg3*△ yeast mutant and its pYES2 empty vector transformed cells could not recover growth on nutrient-rich medium, while transformants with pYES2-*MdATG3a/3b* could resume growth like WT cells (Fig. S2), indicating that both MdATG3a and MdATG3b are functional homologs of yeast Atg3.

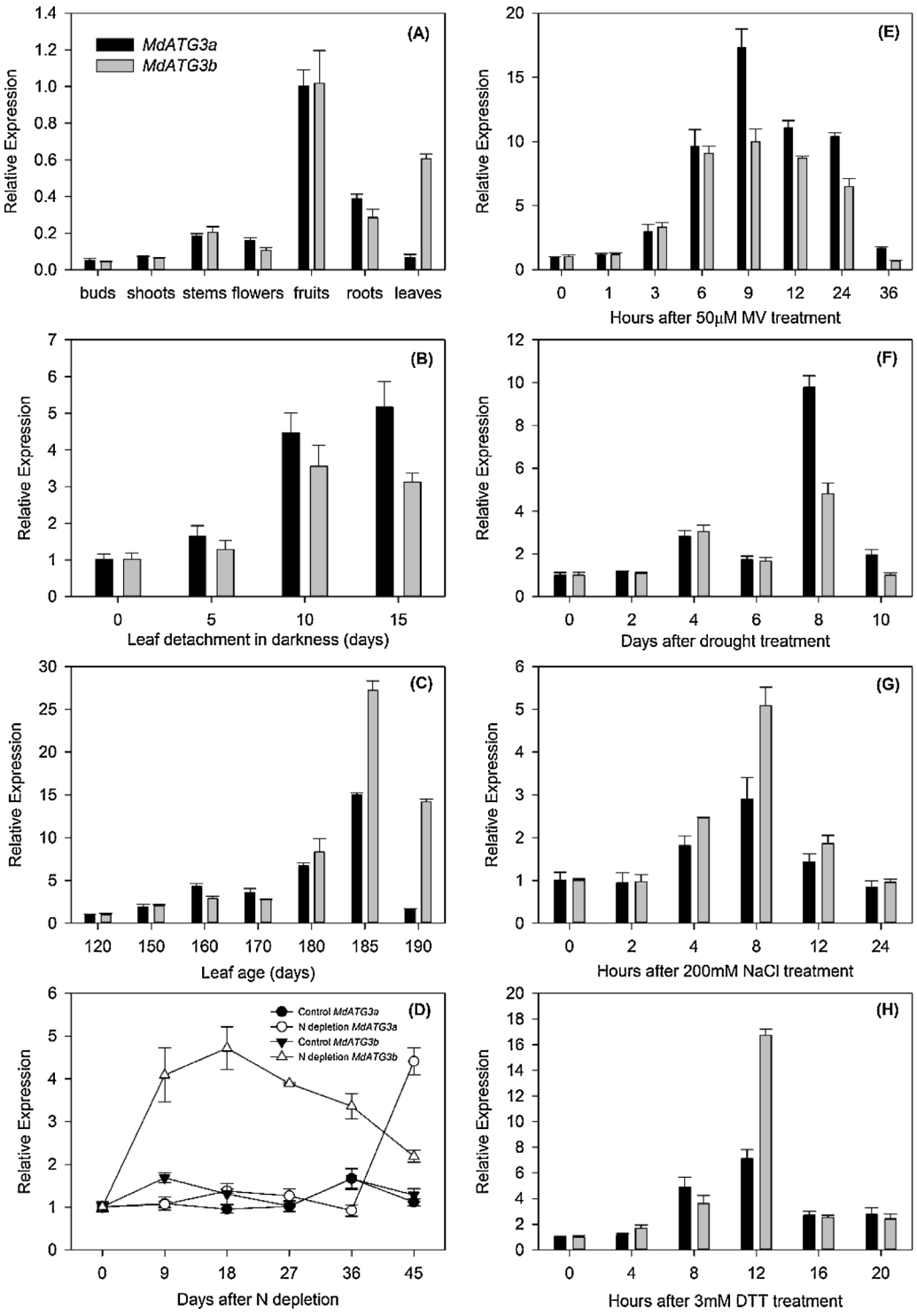

Fig. 3. Expression analysis of *MdATG3a* and *MdATG3b*. Relative expression in different tissues (A), upon dark-induced senescence of detached leaves (B), upon natural leaf senescence (C), during N-depletion treatment (D), in roots exposed to 50 μM MV (E), in leaves after drought treatment (F), in leaves exposed to 200 mM NaCl (G), and in roots after treatment with 3 mM DTT (H). Total RNA was extracted from samples and qRT-PCR was performed with gene-specific primers. Expression levels were calculated relative to expression of *Malus EF-1α* mRNA. Data are means ± SD of 3 technical replicates.

3.5. *Both MdATG3a- and MdATG3b-transgenic* Arabidopsis *facilitate growth and bolting*

We found several stress-responsive cis-elements in the promoters of *MdATG3a* and *MdATG3b*, and both genes were induced to abiotic stress transcriptionally (Fig. 2; Fig. 3). To further study the potential functioning of *MdATG3a* and *MdATG3b* during growth and in response to abiotic stress, we analyzed the phenotype of overexpressing (OE) *Arabidopsis* plants under control of the CaMV 35S promoter. For each gene, we selected two independent T_3 homozygous lines (*MdATG3a* OE2 and OE3; *MdATG3b* OE4 and OE11) that showed high expression, based on PCR analysis in gDNA and cDNA (Fig. S3).

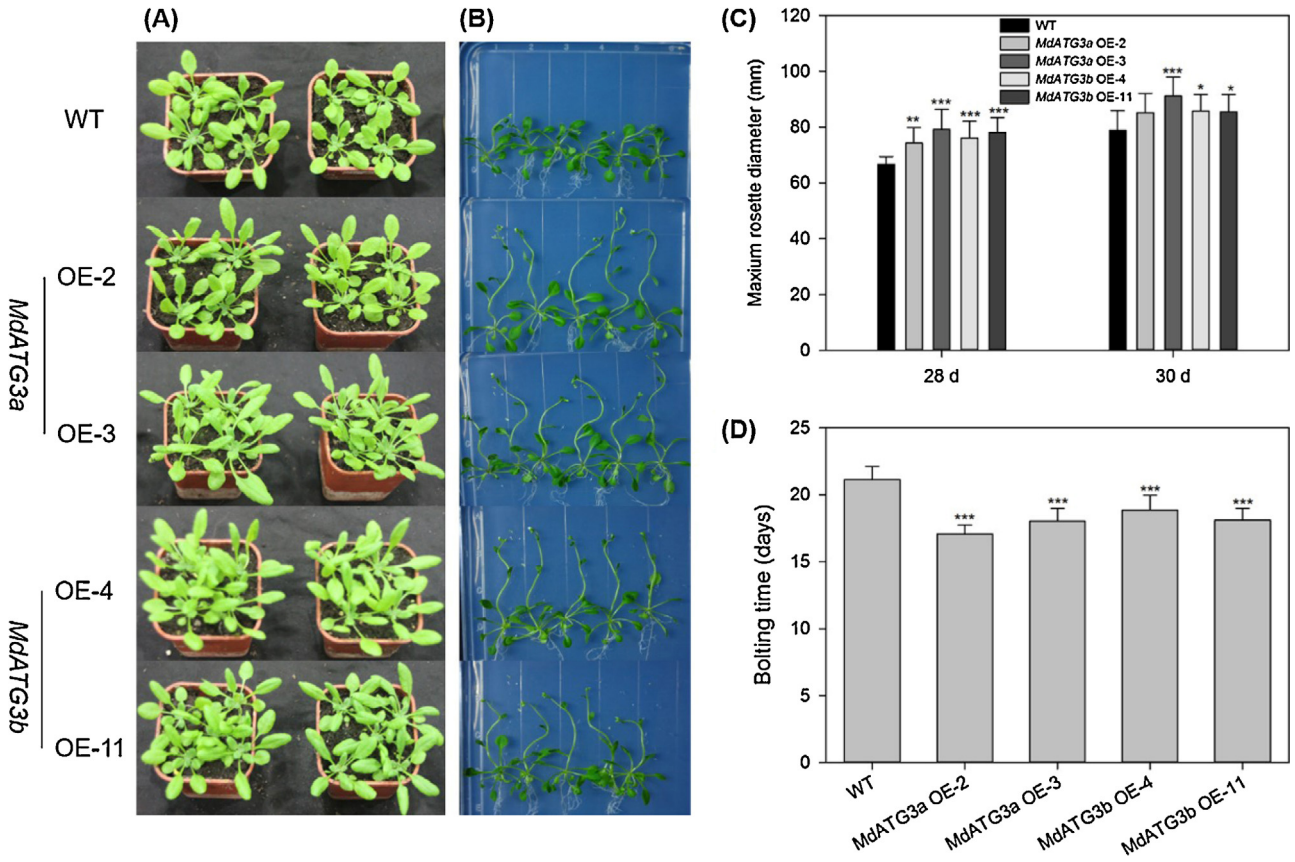

Fig. 4. Overexpression of *MdATG3a* or *MdATG3b* in *Arabidopsis* accelerates growth and bolting. (A) Growth performance of 30-day-old seedlings in soil under LD conditions. (B) Comparisons of bolting times among 25-day-old seedling in MS plates under LD conditions. (C) Maximum rosette diameters of seedlings growing in soil under LD for 28 and 30 d. Data are means ± SD of 20 plants. (D) Statistical analysis of bolting time. Data are means ± SD of 18 plants. *, **, and *** indicate statistically significant differences, as determined by Student's *t*-tests, at $P < 0.05$, $P < 0.01$, and $P < 0.001$, respectively.

Under LD conditions, both *MdATG3a*- and *MdATG3b*-transgenic *Arabidopsis* seedlings grew faster and had larger rosette diameters than WT at Days 28 and 30 (Fig. 4A, C). And these transgenics growing in pots bolted earlier and had higher main inflorescence than the WT at Day 40 (Fig. S4). To investigate bolting time more thoroughly, we sterilized seeds and placed them on a standard MS medium under LD conditions for 25 d, and found that the *MdATG3a*- and *MdATG3b*-transgenic seedlings bolted significantly earlier, with an average of 3 d before the WT (Fig. 4B, D). No differences in growth performance were obvious among the OE lines.

3.6. *Both MdATG3a- and MdATG3b confer tolerance to abiotic stresses in transgenic* Arabidopsis

Because *MdATG3a* and *MdATG3b* were induced by different types of abiotic stresses, we tested the responses of OE lines to 200 mM mannitol, 100 mM NaCl, or N-/C-starvation. When 7-day-old seedlings were exposed to mannitol or NaCl for 15 d, both the *MdATG3a*- and *MdATG3b*-transgenic lines had better growth performance than the WT (Fig. 5A), as shown by their significantly higher fresh weights (Fig. 5B) and longer roots (Fig. 5C). We also noticed that the transgenic plants had longer inflorescences when grown on MS control plates (Fig. 5A). This probably could explain their significantly greater biomass production (Fig. 5B) and earlier bolting when compared with the WT (Fig. 4B, D).

After 5-day-old seedlings were transferred to N-depletion media or both N- and sugar- depletion media for 10 d, the cotyledons of both WT and OE lines turned yellow (Figs. 6 A, S5A). However, their meristems were obviously different, with transgenic plants producing more and larger true leaves (Figs. 6A, S5A). Furthermore, fresh weights and root lengths were noticeably greater when compared with the WT (Figs. 6B, C; S5B, C). After 25 d of N-starvation treatment, the WT plants had died but transgenic plants still had green and living meristems (Fig. 6A). However, N/Sugar depletion treatment exhibited this phenotype more earlier and severer than sole N-depleted treatment. At Day 17, the leaves from WT became white and transparent, while that from transgenic lines still remained two green true leaves (Fig. S5A). This phenotype indicated that overexpression of *MdATG3a* or *MdATG3b* in *Arabidopsis* could improve tolerance to N depletion or N/Sugar depletion.

We also evaluated the recovery growth of *Arabidopsis* after C-starvation, exposing 7-day-old seedlings to either MS or sugar-depletion media for 10 d in the dark before returning them to LD conditions for another 10 d. For both types of media, OE lines showed better recovery, as evidenced by their better fresh weights and numbers of true leaves produced (Fig. 7). However, the root systems of these various genotypes did not grow uniformly, and differences in root lengths were not apparent among the OE lines and the WT. This recovery phenotype was also confirmed by incubating 14-day-old seedlings on MS plates under darkness for another 14 d before resuming growth under LD conditions. After 8 d of exposure to light, numerous WT plants had wilted and died while most OE plants had recovered their growth rate and displayed new green leaves (Fig. S6). These results supported our conclusion that both *MdATG3a* and *MdATG3b* could enhance the recoverability from C-starvation when growing conditions became favorable again.

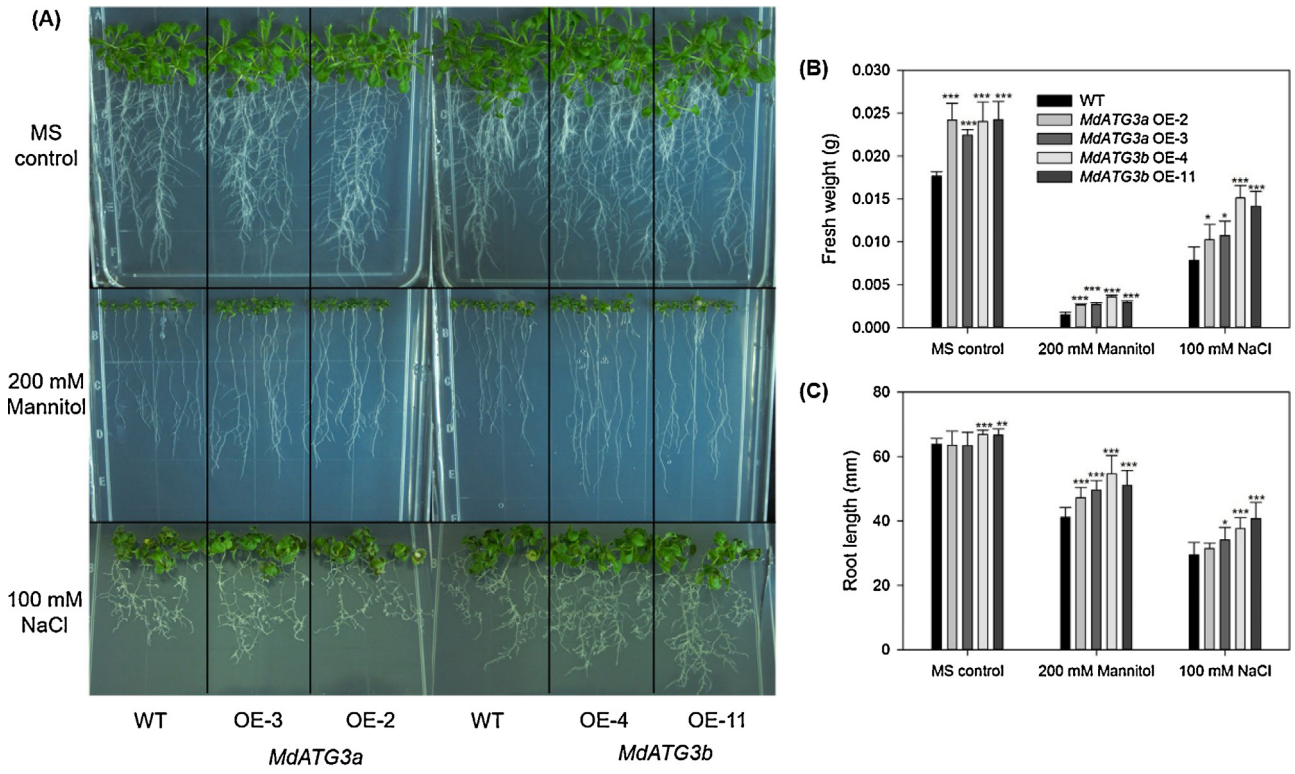

Fig. 5. Overexpression of *MdATG3a* or *MdATG3b* in *Arabidopsis* enhances tolerance to mannitol or NaCl. (A) Growth comparisons among WT and OE lines under MS control, 200 mM mannitol, or 100 mM NaCl treatment for 15 d. (B) Fresh weights. (C) Root lengths. Data are means ± SD of 15 plants. *, **, and *** indicate statistically significant differences, as determined by Student's *t*-tests, at $P < 0.05$, $P < 0.01$, and $P < 0.001$, respectively.

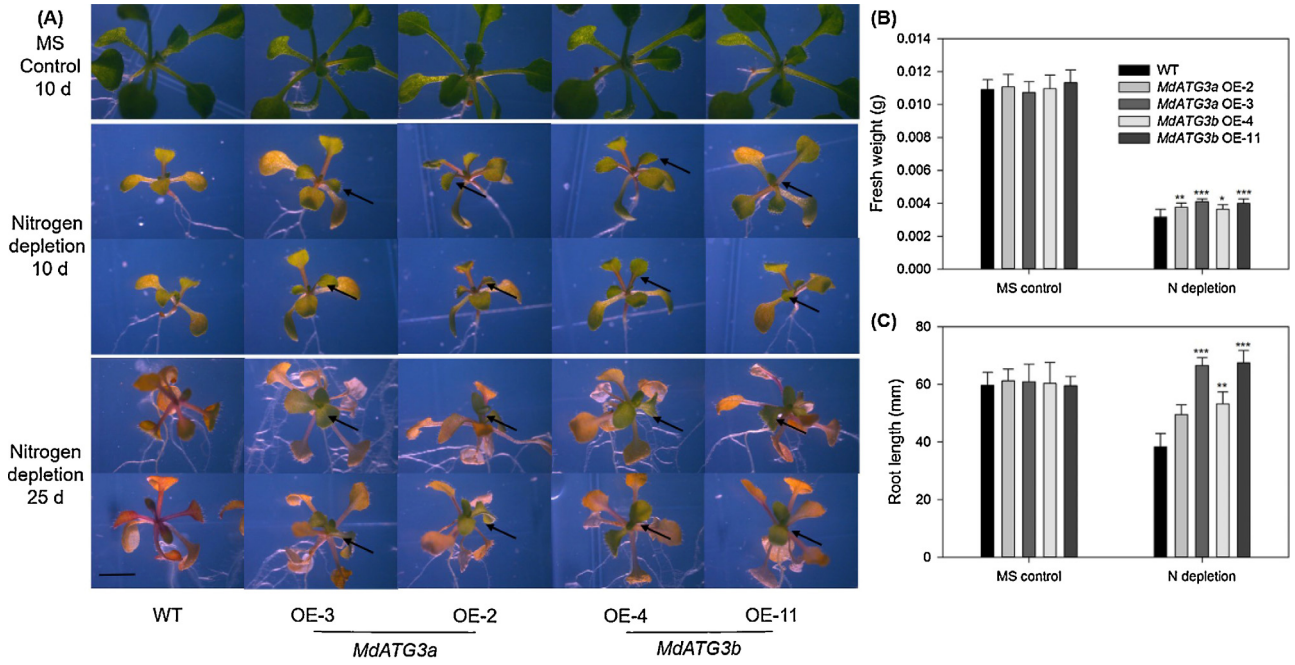

Fig. 6. Overexpression of *MdATG3a* or *MdATG3b* in *Arabidopsis* enhances tolerance to nitrogen depletion. (A) Growth comparisons among WT and OE lines under MS control or N-starvation for 10 or 25 d under LD conditions. (B) Fresh weights. (C) Root lengths. Black arrowheads indicate living and green true leaves. Scale bar = 5 mm. Data are means ± SD of 15 plants. *, **, and *** indicate statistically significant differences, as determined by Student's *t*-tests, at $P < 0.05$, $P < 0.01$, and $P < 0.001$, respectively. (For interpretation of the references to colour in this figure legend, the reader is referred to the web version of this article.)

In general, these performances by *MdATG3a* and *MdATG3b* OE *Arabidopsis* plants not only demonstrated the functional redundancy of those genes, but also suggested their potential for improving plant tolerance toward different abiotic stresses.

3.7. *MdATG3b*-transgenic 'Orin' apple callus shows improved growth performance when nutrient supplies are limited

Three transgenic 'Orin' apple lines over-expressing *MdATG3b* were confirmed by PCR with gDNA (Fig. 8A) and by qRT-PCR with

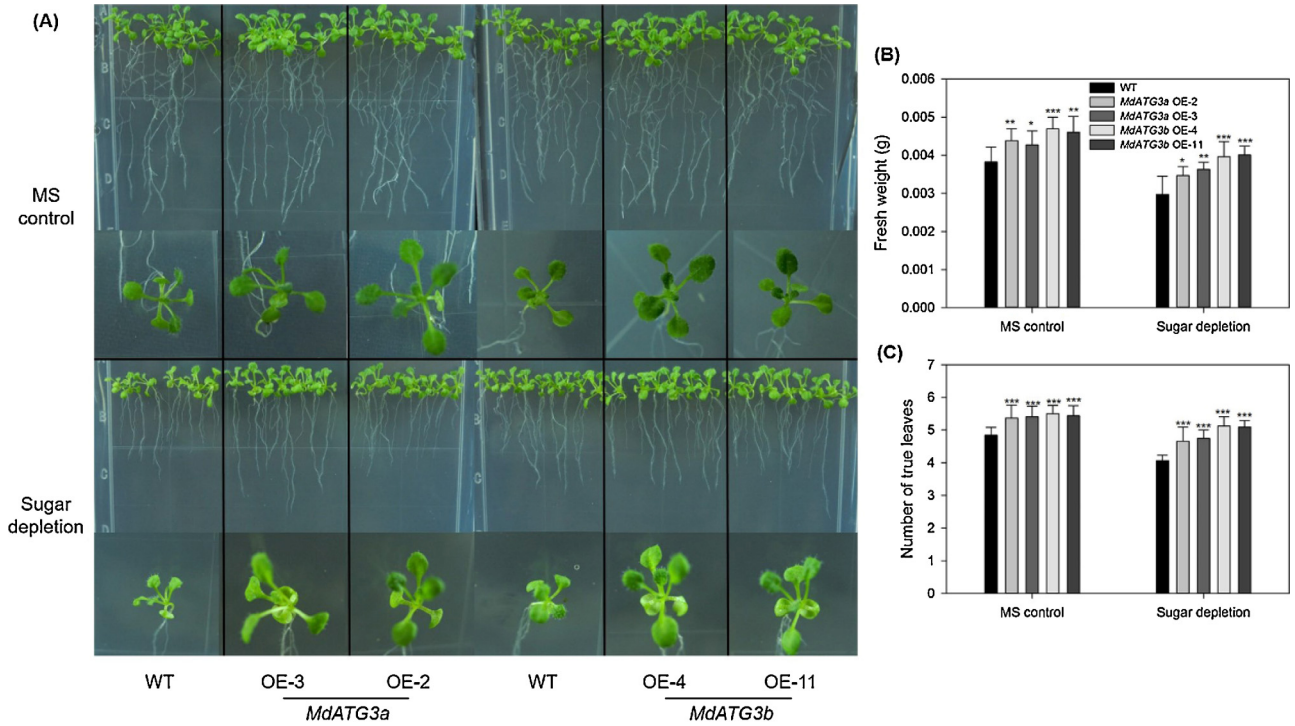

Fig. 7. Overexpression of *MdATG3a* or *MdATG3b* in *Arabidopsis* improves recovery after sugar depletion. (A) Comparisons of 10-d growth recovery among WT and OE lines under MS control or C-starvation for 10 d under LD conditions. (B) Fresh weights. (C) Numbers of true leaves. Data are means ± SD of 15 plants. *, **, and *** indicate statistically significant differences, as determined by Student's *t*-tests, at $P < 0.05$, $P < 0.01$, and $P < 0.001$, respectively.

cDNA (Fig. 8B). The mRNA transcript levels were increased by 25-, 19-, and 24-fold in Lines OE-10, OE-11, and OE-14, respectively (Fig. 8B). For further tests, 14-day-old fresh calli of similar size (~0.02 g) were transferred to MS control, low-sugar, or low-N media. After 20 d of treatment, the callus on the control medium was similar in growth status and weight to all transgenic lines except OE-11, for which the callus was smaller than the WT and other OE lines (Fig. 8C, D). On the low-sugar media, the three transgenic lines had better growth and were significantly heavier than the WT (Fig. 8C, D). Under low-N conditions, the WT callus turned white and stopped growing while calli from the three OE lines remained yellow and showed better growth (Fig. 8C, D). These results demonstrated that, at the cellular level, overexpression of *MdATG3b* could improve growth performance when either C or N were limited.

4. Discussion

Investigating the molecular realm of autophagy began with the identification of *ATG* genes [37]. Many of those genes that are required for autophagosome formation, i.e., the 'core' autophagy machinery, are conserved in eukaryotes. As one of the major groups within that machinery, the ATG8-PE ubiquitin-like conjugation system essentially functions during expansion of the autophagosome membrane [38] and for specific cargo selection by interacting with receptors [7]. In that system, ATG3 receives ATG8 from ATG7 and transfers it to PE, acting as an E2-like enzyme to catalyze protein–lipid conjugation, in contrast to other E2 enzymes [25]. We found here that both *MdATG3a* and *MdATG3b* had conserved N-terminal, catalytic, and C-terminal domains of autophagy-related protein 3. The N-terminal region is critical to autophagy because it forms an amphipathic helix and binds membranes with high curvature [25,39]. The catalytic domain of MdATG3s contains a conserved cysteine residue (Cys^{253}) within the "HPC" motif. Conservation of this residue is a characteristic feature of autophagic E2-like enzymes, including Atg3 and Atg10 homologs from various eukaryotic cells [10,40]. Cysteine is also the only active residue that is universally conserved in the spectrum of E2 and E2-like enzymes in eukaryotes [40,41]. In Atg10, it is essential for recognizing the Apg5 subunit of the autophagosome complex [42]. The small C-terminal domain is likely a distinct binding region that stabilizes the autophagosome [43]. In yeast, Atg3 can directly interact with Atg8 through the WXXL sequence, a canonical Atg8 family interacting motif (AIM) that is crucial for the transfer of Atg8 from the Atg8-Atg3 thioester intermediate to PE [44]. According to the very recent paper [45], the conserved DKYLFL motif between apple and *Arabidopsis* was predicted to act as WXXL-like motif to interact with AtATG8F in *Arabidopsis*. In this study, Y2H assays showed that MdATG3s could interact with MdATG8i in yeast as well. This suggested their involvement in the ATG8 conjugation system in a conserved mechanism. Therefore, the highly conserved sequences and similarity between *MdATG3a* and *MdATG3b* implied that they have similar functions, as reflected by complementation assay in *atg3*△ yeast mutant and plant performances under normal growing conditions as well as in response to abiotic stresses.

We isolated the promoter regions of both genes from apple genomic DNA. The *cis*-acting elements in the promoters were bioinformatically analyzed to predict potential regulatory mechanisms of gene expression in response to environmental stresses or hormone signaling. Both have the drought-responsive element MBS, defense- and stress-responsive element TC-rich repeats, and heat-responsive element HSE. This suggests that the *MdATG3*s are involved in responses to drought, defense, and heat that have been addressed by other autophagy genes [16,22,46]. Several motifs or elements involved in GA_3-, SA-, MeJA-, or ethylene-responsiveness might also participate in stress responses or development processes. The Skn-1_motif and GCN4_motif, which are required for endosperm expression, are also found in the promoters of both genes. Therefore, these *cis*-element predictions in the *MdATG3s* promoter regions might be essential for mediating responses to stress

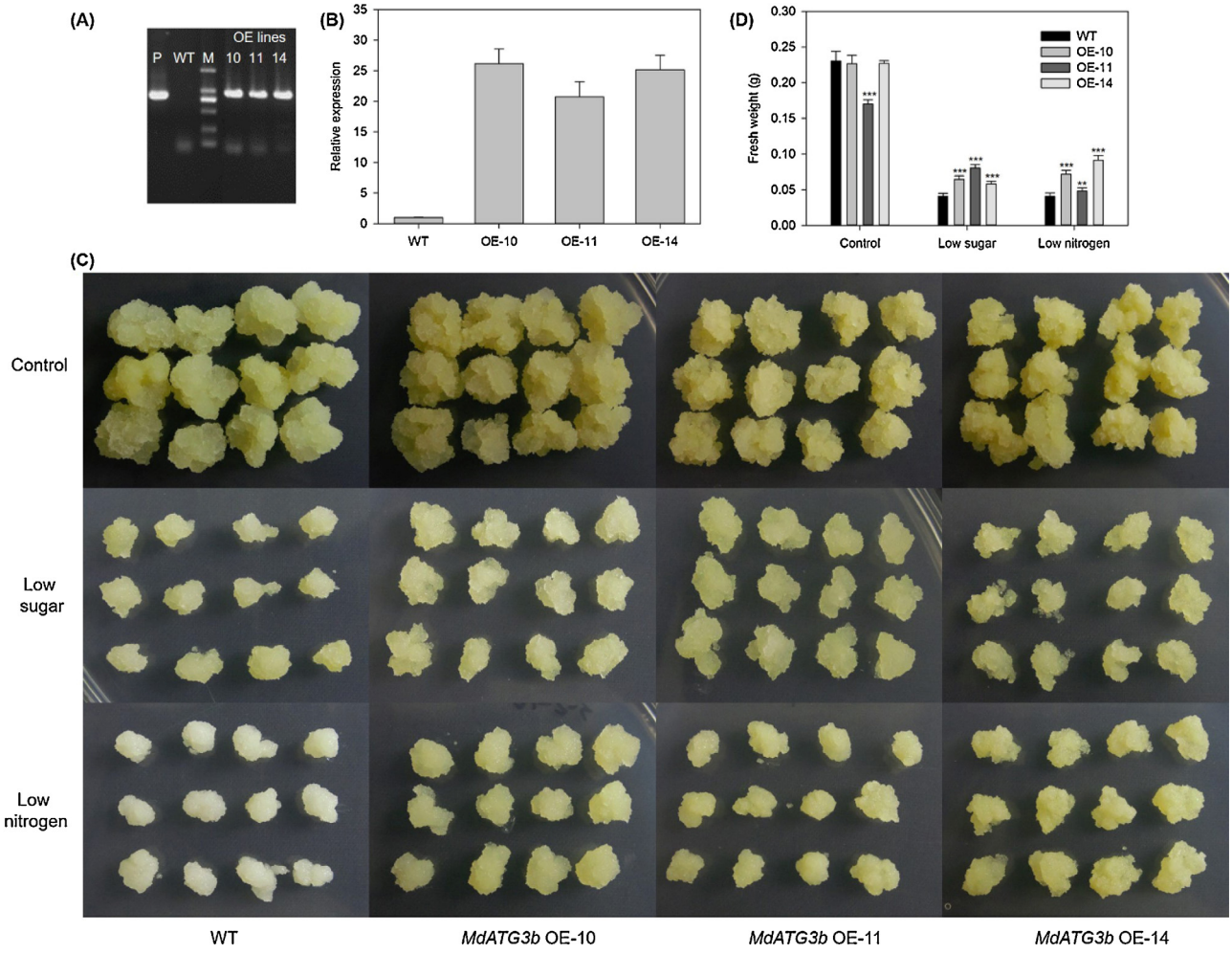

Fig. 8. Overexpression of *MdATG3b* in 'Orin' apple callus improves growth when nitrogen or sugar supplies are limited. (A) PCR-verification of constitutive expression. Lanes M, molecular marker DL2000; P, positive plasmid pCambia2300–*MdATG3b*; WT, non-transformed wild-type; and OE-10, −11, −14 transgenic lines. (B) qRT-PCR analysis of *MdATG3b* expression in WT and transgenic lines. (C) Morphology of calli after 20 d of treatment. (D) Fresh weights of calli after 20 d. Data are means ± SD of 3 biological replicates. *, **, and *** indicate statistically significant differences, as determined by Student's *t*-tests, at $P < 0.05$, $P < 0.01$, and $P < 0.001$, respectively.

and hormones as well as during normal phases of plant growth and development.

Senescence occurs in aging, stressed, or detached leaves and is accompanied by macromolecule degradation and nutrient-recycling [47]. As one of the pathways contributed to degradation, autophagy is involved in senescence and plays an important role in nutrient remobilization. There were nineteen *Arabidopsis ATG* genes that are markedly activated at the transcriptional level, and most of them appear to be coordinately up-regulated at a stage in developmental senescence when chlorophyll degradation becomes visible [48]. Consistently, we have found that *MdATG3a* and *MdATG3b* are up-regulated during both natural and detachment-induced leaf senescence. We have also previously reported that other *ATG*s isolated from *M. domestica* are greatly up-regulated during leaf senescence [23,24,49].

Autophagy is a biological process thought to be a central component in the integrated stress response [2]. Because ROS are toxic and reactive, they may damage cell components, including proteins and nucleic acids. In mammalian cells, an increase in ROS accumulations is often associated with the activation of mitogen-activated protein kinases, including JNK, which can stimulate autophagy [50,51]. Treatment with MV, as well the induction of osmotic or salt stress, can lead to the production of ROS and create oxidative damage in plant cells [11]. When *Arabidopsis* seedlings are exposed to oxidative stress by the addition of H_2O_2 or MV, autophagy is rapidly and strongly induced [15]. Likewise, we found that *MdATG3a* and *MdATG3b* were responsive to MV-induced oxidative stress, drought, and salinity, and their expression patterns were similar at the transcriptional level. Moreover, our *Arabidopsis* OE lines exhibited improved plant tolerance to mannitol-induced osmotic stress and salinity. These results implied that this heightened tolerance might be due to the activation of autophagy when the *MdATG3*s from apple were over-expressed in transgenic *Arabidopsis*. We have previously shown that *MdATG7b* can increase seed germination rates under mild salinity stress when heterologously expressed in *Arabidopsis* [23]. Reports have also been made that *AtATG18a* is required for conferring tolerance to drought and salt stress [16], and that *OsATG10b* plays an important role in the survival of rice cells against oxidative stresses [18]. Research on the regulation of autophagy in *Lycopersicon esculentum* has revealed that a heat-shock transcription factor, *HsfA1a*, confers drought tolerance by activating *ATG* genes and inducing autophagy [46]. Therefore, under oxidative stress, one possible function of autophagy might be the degradation of oxidized or ubiquitinated protein aggregates, thereby protecting cells and supporting plant survival [14,15,46].

Genetic analyses with yeast, mammalian cells, and *Arabidopsis* have demonstrated that autophagy is the major contributor to the recycling of intracellular constituents and, thus, is critical for alleviating nutrient stress [7,8,52]. We found here that both *MdATG3a* and

MdATG3b were up-regulated in N-starved *M. hupehensis* seedlings, although their expression patterns differed. This is consistent with results from studies of *Arabidopsis ATG* genes upon sucrose starvation [12], *ATG8*s from *Glycine max* (soybean) under nitrogen deficiency [53], and most of the *ATG* genes from *Hordeum vulgare* when induced by an N-limitation [54]. Overexpression of *MdATG3a* or *MdATG3b* in *Arabidopsis* facilitates the growth and vigor of meristems either during periods of N-starvation or when plants are recovering after sucrose starvation. Although we over-expressed only *MdATG3b* in our 'Orin' apple callus, all of those transgenic lines performed better than the WT when C or N was less available. These findings are consistent with our previous results with *MdATG8i* [23] or those reported from a study of *GmATG8c* in soybean [53]. Our earlier investigation with *MdATG8i* or *MdATG7*, together with *MdATG3*s in the ATG8-PE conjugation system, indicated that nutrient-deprived tissues had the same degree of improvement after those genes were over-expressed, whether *Arabidopsis* or apple calli were used in the tests [23,24]. This suggested that the core genes for ATG8-PE conjugation worked synergistically. Furthermore, the high homology and similar performance between *MdATG3a* and *MdATG3b* implies that both have functional redundancy.

In conclusion, we have isolated two *ATG3* homologs – *MdATG3a* and *MdATG3b* – from apple. They are similar in their sequences, *cis*-acting elements in the promoters, and expression patterns in response to leaf senescence and abiotic stresses. Both genes also confer greater tolerance to abiotic stresses via heterologous expression when *Arabidopsis* or apple callus is examined. When combined with the knowledge gained from earlier investigations with *MdATG8i* and *MdATG7* in apple, we believe that over-expressing important *ATG* genes in the ATG8-PE conjugation system could improve plant performance and tolerance to various stresses.

Author contributions

P.W. and F.W.M. designed the experiments and financially support the project; P.W. and X.S. performed the experiments; X.J. was involved in collecting data; P.W. wrote the manuscript; and F.W.M. critically revised the article.

Acknowledgments

This work was supported by the Young Scientists Fund of the National Natural Science Foundation of China (31601735) and by the earmarked fund for the China Agriculture Research System (CARS-28). The authors have no conflict of interest to declare.

Appendix A. Supplementary data

Supplementary data associated with this article can be found, in the online version, at http://dx.doi.org/10.1016/j.plantsci.2016.12.003.

References

[1] R. Mittler, Abiotic stress, the field environment and stress combination, Trends Plant Sci. 11 (2006) 15–19.
[2] G. Kroemer, G. Marino, B. Levine, Autophagy and the integrated stress response, Mol. Cell 40 (2010) 280–293.
[3] C. He, D.J. Klionsky, Regulation mechanisms and signaling pathways of autophagy, Annu. Rev. Genet. 43 (2009) 67–93.
[4] X. Liu, F. Xu, J.H. Snyder, H. Shi, J. Lu, F. Lin, Autophagy in plant pathogenic fungi, Semin, Cell Dev. Biol. (2016) 128–137.
[5] Z. Yang, D.J. Klionsky, Mammalian autophagy: core molecular machinery and signaling regulation, Curr. Opin. Cell Biol. 22 (2010) 124–131.
[6] M. Mehrpour, A. Esclatine, I. Beau, P. Codogno, Overview of macroautophagy regulation in mammalian cells, Cell Res. 20 (2010) 748–762.
[7] F. Li, R.D. Vierstra, Autophagy: a multifaceted intracellular system for bulk and selective recycling, Trends Plant Sci. 17 (2012) 526–537.
[8] Y. Liu, D.C. Bassham, Autophagy: pathways for self-eating in plant cells, Annu. Rev. Plant Biol. 63 (2012) 215–237.
[9] Y. Ichimura, Y. Imamura, K. Emoto, M. Umeda, T. Noda, Y. Ohsumi, *In vivo* and *in vitro* reconstitution of Atg8 conjugation essential for autophagy, J. Biol. Chem. 279 (2004) 40584–40592.
[10] Y. Yamada, N.N. Suzuki, T. Hanada, Y. Ichimura, H. Kumeta, Y. Fujioka, Y. Ohsumi, F. Inagaki, The crystal structure of Atg3, an autophagy-related ubiquitin carrier protein (E2) enzyme that mediates Atg8 lipidation, J. Biol. Chem. 282 (2007) 8036–8043.
[11] S. Han, B. Yu, Y. Wang, Y. Liu, Role of plant autophagy in stress response, Protein Cell 2 (2011) 784–791.
[12] T.L. Rose, L. Bonneau, C. Der, D. Marty-Mazars, F. Marty, Starvation-induced expression of autophagy-related genes in Arabidopsis, Biol. Cell 98 (2006) 53–67.
[13] Y. Chen, M.B. Azad, S.B. Gibson, Superoxide is the major reactive oxygen species regulating autophagy, Cell Death Differ. 16 (2009) 1040–1052.
[14] Y. Xiong, A.L. Contento, D.C. Bassham, Disruption of autophagy results in constitutive oxidative stress in *Arabidopsis*, Autophagy 3 (2007) 257–258.
[15] Y. Xiong, A.L. Contento, P.Q. Nguyen, D.C. Bassham, Degradation of oxidized proteins by autophagy during oxidative stress in *Arabidopsis*, Plant Physiol. 143 (2007) 291–299.
[16] Y. Liu, Y. Xiong, D.C. Bassham, Autophagy is required for tolerance of drought and salt stress in plants, Autophagy 5 (2009) 954–963.
[17] S. Slavikova, S. Ufaz, T. Avin-Wittenberg, H. Levanony, G. Galili, An autophagy-associated Atg8 protein is involved in the responses of *Arabidopsis* seedlings to hormonal controls and abiotic stresses, J. Exp. Bot. 59 (2008) 4029–4043.
[18] J.H. Shin, K. Yoshimoto, Y. Ohsumi, J.S. Jeon, G. An, OsATG10b, an autophagosome component, is needed for cell survival against oxidative stresses in rice, Mol. Cells 27 (2009) 67–74.
[19] Y. Liu, J.S. Burgos, Y. Deng, R. Srivastava, S.H. Howell, D.C. Bassham, Degradation of the endoplasmic reticulum by autophagy during endoplasmic reticulum stress in *Arabidopsis*, Plant Cell 24 (2012) 4635–4651.
[20] X. Yang, R. Srivastava, S.H. Howell, D.C. Bassham, Activation of autophagy by unfolded proteins during endoplasmic reticulum stress, Plant J. 85 (2016) 83–95.
[21] J. Zhou, J. Wang, Y. Cheng, Y.J. Chi, B. Fan, J.Q. Yu, Z. Chen, NBR1-mediated selective autophagy targets insoluble ubiquitinated protein aggregates in plant stress responses, PLoS Genet. 9 (2013) e1003196.
[22] J. Zhou, J. Wang, J.Q. Yu, Z. Chen, Role and regulation of autophagy in heat stress responses of tomato plants, Front. Plant Sci. 5 (2014) 174.
[23] P. Wang, X. Sun, X. Jia, N. Wang, X. Gong, F. Ma, Characterization of an autophagy-related gene *MdATG8i* from apple, Front. Plant Sci. 7 (2016) 720.
[24] P. Wang, X. Sun, N. Wang, X. Jia, F. Ma, Ectopic expression of an autophagy-associated MdATG7b gene from apple alters growth and tolerance to nutrient stress in *Arabidopsis thaliana*, PCTOC (2016) 1–15.
[25] T. Hanada, Y. Satomi, T. Takao, Y. Ohsumi, The amino-terminal region of Atg3 is essential for association with phosphatidylethanolamine in Atg8 lipidation, FEBS Lett. 583 (2009) 1078–1083.
[26] P. Wang, L. Yin, D. Liang, C. Li, F. Ma, Z. Yue, Delayed senescence of apple leaves by exogenous melatonin treatment: toward regulating the ascorbate-glutathione cycle, J. Pineal Res. 53 (2012) 11–20.
[27] C. Li, P. Wang, Z. Wei, D. Liang, C. Liu, L. Yin, D. Jia, M. Fu, F. Ma, The mitigation effects of exogenous melatonin on salinity-induced stress in *Malus hupehensis*, J. Pineal Res. 53 (2012) 298–306.
[28] X. Ma, F. Ma, Y. Mi, Y. Ma, H. Shu, Morphological and physiological responses of two contrasting *Malus* species to exogenous abscisic acid application, Plant Growth Regul. 56 (2008) 77–87.
[29] H. Hanaoka, T. Noda, Y. Shirano, T. Kato, H. Hayashi, D. Shibata, S. Tabata, Y. Ohsumi, Leaf senescence and starvation-induced chlorosis are accelerated by the disruption of an *Arabidopsis* autophagy gene, Plant Physiol. 129 (2002) 1181–1193.
[30] T. Chung, R.P. Allison, R.D. Vierstra, ATG8 lipidation and ATG8-mediated autophagy in *Arabidopsis* require ATG12 expressed from the differentially controlled *ATG12A* and *ATG12B* loci, Plant J. 62 (2010) 483–493.
[31] G. Gambino, I. Perrone, I. Gribaudo, A rapid and effective method for RNA extraction from different tissues of grapevine and other woody plants, Phytochem. Anal. 19 (2008) 520–525.
[32] S. Porebski, L.G. Bailey, B.R. Baum, Modification of a CTAB DNA extraction protocol for plants containing high polysaccharide and polyphenol components, Plant Mol. Biol. Rep. 15 (1997) 8–15.
[33] T. Liu, Expression Pattern and Functional Analysis of an Autophagy-related Gene MgATG4 in *Magnaporthe oryzae*, Dissertation, Zhejiang University, 2008.
[34] X. Zhang, R. Henriques, S.S. Lin, Q. Niu, N.H. Chua, Agrobacterium-mediated transformation of Arabidopsis thaliana using the floral dip method, Nat. Protoc. 1 (2006) 641–646.
[35] X. Xie, S. Li, R. Zhang, J. Zhao, Y. Chen, Q. Zhao, Y. Yao, C. You, X. Zhang, Y. Hao, The bHLH transcription factor MdbHLH3 promotes anthocyanin accumulation and fruit colouration in response to low temperature in apple, Plant Cell Environ. 35 (2012) 1884–1897.
[36] Y. Ichimura, T. Kirisako, T. Takao, Y. Satomi, Y. Shimonishi, N. Ishihara, N. Mizushima, I. Tanida, E. Kominami, M. Ohsumi, T. Noda, Y. Ohsumi, A ubiquitin-like system mediates protein lipidation, Nature 408 (2000) 488–492.

[37] D.J. Klionsky, J.M. Cregg, W.A. Dunn, S.D. Emr, Y. Sakai, I.V. Sandoval, A. Sibirny, S. Subramani, M. Thumm, M. Veenhuis, Y. Ohsumi, A unified nomenclature for yeast autophagy-related genes, Dev. Cell 5 (2003) 539–545.
[38] H. Nakatogawa, Y. Ichimura, Y. Ohsumi, Atg8 a ubiquitin-like protein required for autophagosome formation, mediates membrane tethering and hemifusion, Cell 130 (2007) 165–178.
[39] S. Nath, J. Dancourt, V. Shteyn, G. Puente, W.M. Fong, S. Nag, J. Bewersdorf, A. Yamamoto, B. Antonny, T.J. Melia, Lipidation of the LC3/GABARAP family of autophagy proteins relies on a membrane-curvature-sensing domain in Atg3, Nat. Cell Biol. 16 (2014) 415–424.
[40] M.D. Flanagan, S.K. Whitehall, B.A. Morgan, An Atg10-like E2 enzyme is essential for cell cycle progression but not autophagy in Schizosaccharomyces pombe, Cell Cycle 12 (2013) 271–277.
[41] A.M. Burroughs, M. Jaffee, L.M. Iyer, L. Aravind, Anatomy of the E2 ligase fold: implications for enzymology and evolution of ubiquitin/Ub-like protein conjugation, J. Struct. Biol. 162 (2008) 205–218.
[42] N. Mizushima, T. Yoshimori, Y. Ohsumi, Mouse Apg10 as an Apg12-conjugating enzyme: analysis by the conjugation-mediated yeast two-hybrid method, FEBS Lett. 532 (2002) 450–454.
[43] N. Mizushima, T. Yoshimori, Y. Ohsumi, Role of the Apg12 conjugation system in mammalian autophagy, Intl. J. Biochem. Cell Biol. 35 (2003) 553–561.
[44] M. Yamaguchi, N.N. Noda, H. Nakatogawa, H. Kumeta, Y. Ohsumi, F. Inagaki, Autophagy-related protein 8 (Atg8) family interacting motif in Atg3 mediates the Atg3-Atg8 interaction and is crucial for the Cytoplasm-to-Vacuole targeting pathway, J. Biol. Chem. 285 (2010) 29599–29607.
[45] Q. Wang, O. Tzfadia, M. Levy, E. Weithorn, H. Peled-Zehavi, T. Van Parys, Y. Van de Peer, G. Galili, hfAIM: a reliable bioinformatics approach for in silico genome-wide identification of autophagy-associated Atg8-interacting motifs in various organisms, Autophagy 12 (2016) 876–887.
[46] Y. Wang, S. Cai, L. Yin, K. Shi, X. Xia, Y. Zhou, J. Yu, J. Zhou, Tomato *HsfA1a* plays a critical role in plant drought tolerance by activating ATG genes and inducing autophagy, Autophagy 11 (2015) 2033–2047.
[47] S. Gan, Mitotic and postmitotic senescence in plants, Sci. Aging Knowl. Environ. (2003) RE7.
[48] E. Van der Graaff, R. Schwacke, A. Schneider, M. Desimone, U.I. Flugge, R. Kunze, Transcription analysis of *Arabidopsis* membrane transporters and hormone pathways during developmental and induced leaf senescence, Plant Physiol. 141 (2006) 776–792.
[49] P. Wang, X. Sun, C. Chang, F. Feng, D. Liang, L. Cheng, F. Ma, Delay in leaf senescence of *Malus hupehensis* by long-term melatonin application is associated with its regulation of metabolic status and protein degradation, J. Pineal Res. 55 (2013) 424–434.
[50] C.H. Wong, K.B. Iskandar, S.K. Yadav, J.L. Hirpara, T. Loh, S. Pervaiz, Simultaneous induction of non-canonical autophagy and apoptosis in cancer cells by ROS-dependent ERK and JNK activation, PLoS One 5 (2010) e9996.
[51] J. Liu, F. Chang, F. Li, H. Fu, J. Wang, S. Zhang, J. Zhao, D. Yin, Palmitate promotes autophagy and apoptosis through ROS-dependent JNK and p38 MAPK, Biochem. Biophys. Res. Commun. 463 (2015) 262–267.
[52] Y. Ohsumi, Historical landmarks of autophagy research, Cell Res. 24 (2014) 9–23.
[53] T. Xia, D. Xiao, D. Liu, W. Chai, Q. Gong, N.N. Wang, Heterologous expression of *Atg8c* from soybean confers tolerance to nitrogen deficiency and increases yield in *Arabidopsis*, PLoS One 7 (2012) e37217.
[54] L. Avila-Ospina, A. Marmagne, F. Soulay, C. Masclaux-Daubresse, Identification of barley (*Hordeum vulgare* L.) autophagy genes and their expression levels during leaf senescence, chronic nitrogen limitation and in response to dark exposure, Agronomy 6 (2016) 15.